*Progress In Electromagnetics Research Letters, Vol. 63, 15–21, 2016*

# Compact Triple-Band Bandstop Filters Using Embedded Capacitors

**Ashwani Kumar[1, *], Anand K. Verma[2, 3], and Qingfeng Zhang[4]**

**Abstract**—This paper presents a design of compact a triple-band bandstop filter (BSF) using embedded chip capacitors. The presented BSF is useful to suppressing the signal frequencies 2.2 GHz, 5.53 GHz and 4.15 GHz from the WLAN and UWB band with attenuation level 33.5 dB, 27.6 dB and 24.9 dB, respectively. The quality factors of the three bands are 5.21, 31.92 and 79.0, respectively. The simulated and measured results are presented to validate the concept. Such BSFs could find application in modern communication systems to suppress the potential interference of the unwanted frequencies from the WLAN and UWB band.

## 1. INTRODUCTION

Nowadays, multifunctional wireless integrated communication systems become more and more important and have been used for miniaturization of the communication equipment. In recent years, lots of works have been done on integrated and multifunctional wireless communication systems. Multi-band bandstop filters play an important role and are tremendously preferred, which can be simultaneously used for stopping different signal frequencies. Some effective methods have been proposed to develop dual-band [1–4] and triple-band bandstop filters [5–12]. However, the design of triple-band bandstop filters (TB-BSFs) and controlling the stopband frequencies within the specified band are difficult. Hence, relatively less works have been done on TB-BSFs [5–12]. Recently, some TB-BSFs are designed by using series LC resonators and admittance inverters [5], T-shaped defected microstrip structure [6], cross coupling stubs [7], square patch resonator [8], defected microstrip structure (DMS) and E-shaped defected ground structure (DGS) with open-loop resonators coupled to the microstrip line [9], U-shaped DGS [10], Hilbert-Fork resonator [11] and by using meander line stepped impedance resonator [12]. Multi-ring complementary split ring resonators (multi-ring CSRRs) [13], and meandered DMS (MDMS) structure [14] have also been utilized to design the Triple-Band BSFs.

These TB-BSFs are very useful for suppressing the spurious signals, but the controls of stopband frequencies are very difficult. Because of this difficulty, these bandstop filters are useful only for the particularly designed frequencies. Recently, frequencies band from 2.0 and 2.2 GHz of the S band has been approved for Mobile Satellite Service (MSS) networks in connection with Ancillary Terrestrial Components (ATC) [15]. The frequency bands 4.15 GHz and 5.22 GHz are used for WLAN band. These three frequencies interfere with the other WLAN and UWB band of frequencies. Therefore, suppressing these frequencies requires a multi-band bandstop filter.

This paper presents the design of a triple-band bandstop filter (TB-BSF) using a C-type slot in the ground plane with embedded chip capacitors. The proposed BSF suppresses the potential interference of the unwanted signal frequencies from the WLAN and UWB band. The simulated and experimental results are finally provided to validate the concept.

*Received 24 May 2016, Accepted 12 August 2016, Scheduled 2 October 2016*

* Corresponding author: Ashwani Kumar (ashwanikumar7@yahoo.com).

[1] Department of Electronics, Sri Aurobindo College, University of Delhi, Malviya Nagar, New Delhi-110017, India. [2] Microwave Research Laboratory, Department of Electronic Science, University of Delhi South Campus, New Delhi-110021, India. [3] Department of Electronics, Macquarie University, NSW, Sydney, Australia. [4] Department of Electrical and Electronics Engineering, South University of Science and Technology of China (SUSTC), 518055, China.

## 2. PARAMETRIC STUDY

The proposed TB-BSF with capacitor loaded C-type slot is shown in Fig. 1(b). The C-type slot is etched in the ground plane of a 50 Ω microstrip line on a Neltech substrate with $\varepsilon_r = 3.2,\ h = 0.762\,\text{mm}$. 3D electromagnetic software, CST Microwave studio 2011, has been used to design the proposed bandstop filters [16]. The unloaded C-type slot (without chip capacitors) resonates at two frequencies *lower resonance frequency* $f_L$ and *upper band resonance frequency* $f_H$, with scaling factor $f_H/f_L \approx 3$. The simulated $|S_{21}|$ responses of the C-type slot with fixed gap $g = 1\,\text{mm}$ and $G = 2\,\text{mm}$ for three different sizes are shown in Fig. 1(c). The lower resonance frequency increases from 3.02 GHz to 5.49 GHz to 7.12 GHz while the upper resonance frequency increases from 9.63 GHz to 16.32 GHz to 22.92 GHz by decreasing the size of the C-type slot from ($d_1^{in} = 13.0\,\text{mm}$, $d_2^{in} = 12.7\,\text{mm}$) to ($d_1^{in} = 7.2\,\text{mm}$, $d_2^{in} = 6.6\,\text{mm}$) to ($d_1^{in} = 5.6\,\text{mm}$, $d_2^{in} = 5.0\,\text{mm}$). For the three different size slots, we have average ratio of $f_H/f_L \approx 3$ (scaling factor). Through the numerical experimentation on the EM simulator CST Microwave Studio, a large number of data has been generated of lower and upper resonance frequencies for different sizes of the C-type slot in ground plane. We have developed empirical expressions to compute approximate sides $d_1^{in}$, $d_2^{in}$ of the C-type slot with the help of curve-fitting. The curve-fitted empirical expressions to compute the approximate sides $d_1^{in}$, $d_2^{in}$ are given in Equations (1) and (2).

$$d_1^{in} = 7 \times 10^{-5}(\lambda_g)^3 - 55 \times 10^{-4}(\lambda_g)^2 + 0.317\lambda_g \tag{1}$$

$$d_2^{in} = 10^{-4}(\lambda_g)^3 - 86 \times 10^{-4}(\lambda_g)^2 + 0.4013\lambda_g \tag{2}$$

where $\lambda_g/\sqrt{\varepsilon_r}$ is the guided wavelength obtained using lower resonance frequency, and $d_1^{in}$, $d_2^{in}$ are the dimensions of the C-type slot. For the lower resonance frequency $f_{L1} = 5.4\,\text{GHz}$, the dimensions of the C-type slot computed using (1) and (2) are $d_1^{in} = 7.2\,\text{mm}$, $d_2^{in} = 6.6\,\text{mm}$. Using these dimensions, the slot provides the slightly changed lower resonance frequency at $f_{L1} = 5.49\,\text{GHz}$ and the upper resonance frequency at $f_{U1} = 16.132\,\text{GHz}$. Here frequency $f_{L1} = 5.4\,\text{GHz}$ has been selected so that by doing scaled down with the scaling factor, we can achieve the lower resonance frequency of the TB-BSF at 1.8 GHz. In the next step, the chip capacitors are embedded in the slot, as shown in Fig. 1(b). The electric field distribution and frequency response of the slot without loading the chip capacitors are shown in Fig. 2 and Fig. 1(c), respectively.

Figure 2 shows the electric field distribution in the slot region for both the lower and upper resonant frequencies. At the lower resonance frequency (*Fundamental mode*), the electric field has one maximum while at the higher resonance *(Third harmonic mode)* that is nearly 3 times the lower one, and we observe three maxima. The electric field concentration in Region-I are higher than Region-II for the fundamental mode. For the third harmonic mode, however, the electric field concentration is more in Region-II than Region-I. These two regions have been used to design the TB-BSF by placing the chip capacitors. Three different chip capacitors are required to design a TB-BSF, and the placement of these capacitors is shown in Fig. 1(b).

Our next task is to lower the resonance frequencies in 1–8 GHz band, say in the WLAN band. For this purpose, we load the C-type slot by chip capacitors as shown in Fig. 1(b). Using an EM-simulator, we shall study below the impact of the capacitors $C_1$ and $C_2'$ for fixed $C_2 = 0.3\,\text{pF}$.

Figure 3 demonstrates the variation of $f_1$, $f_2$ and $f_3$ of the TB-BSF with embedded chip capacitors. Fig. 3(a) presents the decrease of frequency $f_1$ with capacitor $C_2$ for fixed capacitor $C_2' = 0.3\,\text{pF}$. Fig. 3(b) shows the variation of the second resonance frequency with capacitor $C_2$ for fixed capacitor $C_2' = 0.3\,\text{pF}$. Initially, the second resonance frequency is slightly lower, and then it starts increasing to some peak value and finally becomes constant. As soon as the capacitors $C_2$ and $C_2'$ become equal, the *Triple-Band BSF changes to a Dual-Band BSF* with a slight shift in frequency, discussed in detail [4]. Further increasing the value of $C_2'$, the *Dual-Band BSF again splits into a Triple-Band BSF*. Fig. 3(c) shows the gap in frequency ($f_3$). This gap demonstrates the merging of Triple-Band to Dual-Band BSF. Fig. 3 can be used as a *design chart* to design the TB-BSF.

It is interesting to note that before merging in to Dual-Band BSF, the resonance frequency ($f_3$) appears in higher frequency side whereas it appears in the lower frequency axis after merging, as shown in Fig. 4. The shifts of the frequency ($f_3$) in higher and lower frequency regions due to the chip capacitors are shown in Fig. 4. However in both the case the resonance frequency ($f_2$) is almost the same.

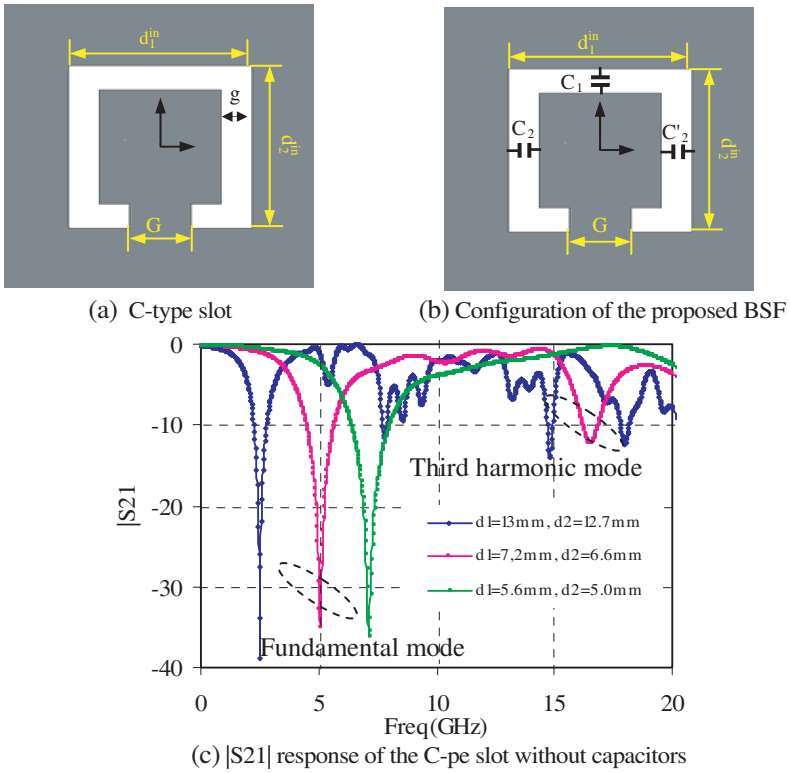


(a) C-type slot (b) Configuration of the proposed BSF

(c) |S21| response of the C-pe slot without capacitors

**Figure 1.** Slot in ground plane (a) C-type slot. (b) BSF Layout with dimensions. (c) $|S_{21}|$ response.

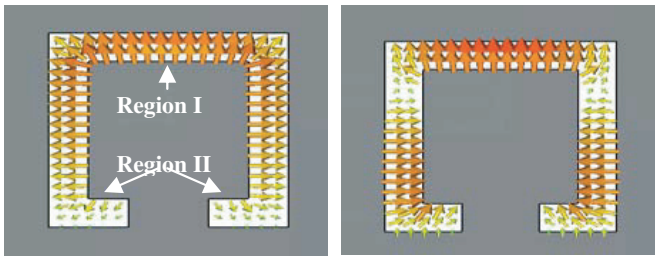


(a) (b)

**Figure 2.** Simulated electric field within the C-type slot in ground plane. (a) Fundamental mode. (b) Third harmonic mode.

## 3. DESIGN AND FABRICATION OF THE TRIPLE-BAND BSF

Figure 3 can be used as a *design chart* to design TB-BSF, as we have already discussed in above section. For the design and fabrication of the TB-BSFs, a Neltech substrate with $\varepsilon_r = 3.2$, $h = 0.762$ mm is used. To verify the design methodology, three TB-BSFs are designed for three different frequencies. For case-1, the specified frequencies of the TB-BSF are ($f_1 = 2.0$ GHz, $f_2 = 5.42$ GHz and $f_3 = 3.86$ GHz), for case-2 ($f_1 = 1.6$ GHz, $f_2 = 5.32$ GHz and $f_3 = 2.94$ GHz) and for case-3 ($f_1 = 2.2$ GHz, $f_2 = 5.53$ GHz and $f_3 = 4.15$ GHz). The *design charts* shown in Fig. 3 are used to obtain these specified frequencies. For case-1, the design chart provides three different capacitance values ($C_1 = 0.8$ pF, $C_2 = 0.3$ pF and $C_2' = 0.9$ pF). For case-2, the three capacitances are ($C_1 = 1.3$ pF, $C_2 = 0.3$ pF and $C_2' = 1.3$ pF). For case-3, the capacitances are ($C_1 = 0.7$ pF, $C_2 = 0.3$ pF and $C_2' = 0.7$ pF). Embedding these capacitors in the C-type slot at positions 1 and 2 as shown in Fig. 1(b) provides the TB-BSFs for these frequencies.

The fractional bandwidth, loaded quality factor and external quality factor are calculated by using

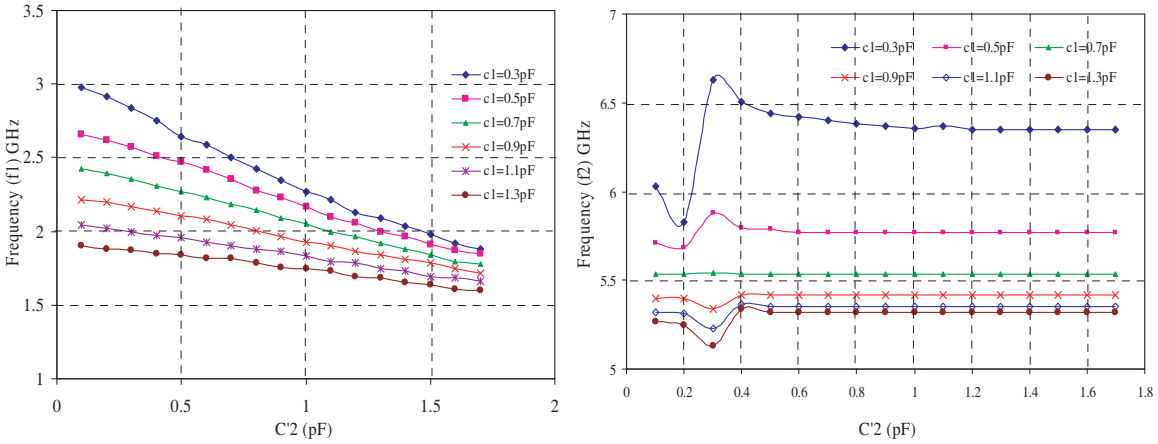


(a) Frequency (f1) variation with C'2 for fixed C2=0.3 pF (b) Frequency (f2) variation with C'2 for fixed C2=0.3 pF

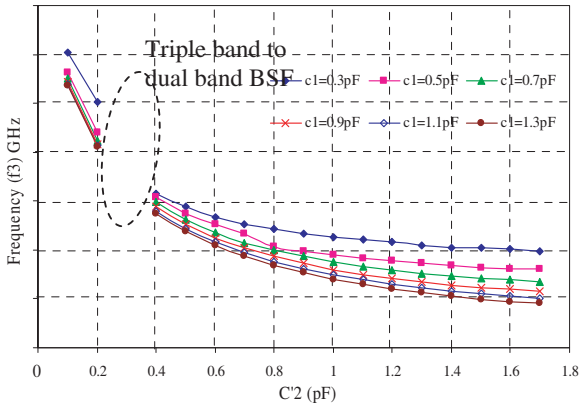


(c) Frequency (f3) variation with C'2 for fixed C2=0.3 pF

**Figure 3.** Design chart for TB-BSF. (a) For frequency ($f_1$). (b) For frequency ($f_2$). (c) For frequency ($f_3$) variation with $C_2'$ for fixed $C_2 = 0.3\,\text{pF}$.

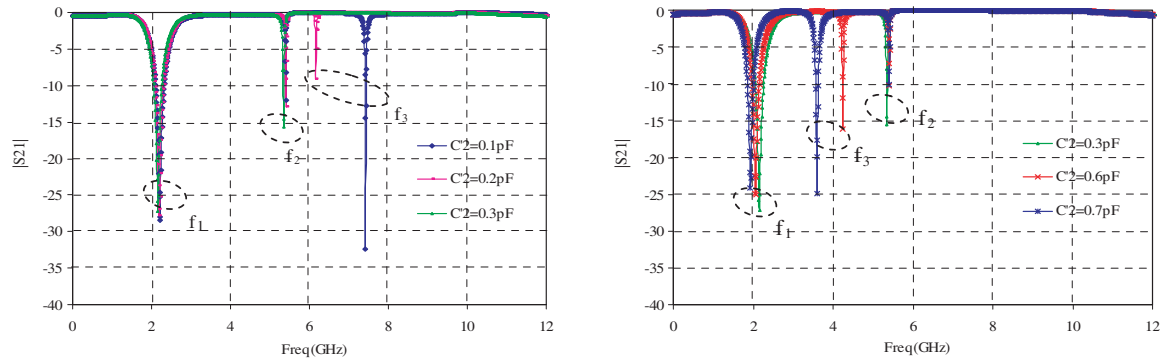


(a) Shift in frequency (f3) and frequency (f2) is almost same (b) Shift in frequency (f1) and frequency (f2) is almost same

**Figure 4.** Show the shift in frequency ($f_3$) in higher and lower frequency region with chip capacitors.

Eqs. (3) to (4).

$$FBW = \frac{f_{\max} - f_{\min}}{f_0} \tag{3}$$

$$Q_L = \frac{f_0}{f_{\max} - f_{\min}} = \frac{f_0}{3\,\text{dB BW}} \tag{4}$$

where $f_{\max}$ and $f_{\min}$ are the 3 dB frequencies, and $f_0$ is the resonance frequency.

The frequency responses of the TB-BSFs for these three cases are illustrated in Fig. 5, Fig. 6 and Fig. 7. Note that the return losses (RL) between the stop bands are: 17.2 dB $\sim$ 19 dB for case-1, 16.2 dB $\sim$ 20 dB for case-2 and 15.2 $\sim$ 22 dB for case-3. The insertion losses (ILs) are: 0.04 $\sim$ 0.07 dB for case-1, 0.05 $\sim$ 0.06 dB for case-2 and 0.08 $\sim$ 0.09 dB for case-3. The performance of the proposed TB-BSFs are compared with the earlier published work, as shown in Table 1. Our all three filters are compact against the reported filters, and the control on stopband is relatively easy. The loaded quality factors of our proposed filters are higher than the reported filter in [5–14]. The fabricated prototype is presented in Fig. 8.

**Table 1.** Performance of triple band BSF.

| Ref. | Frequency (GHz) | | | F.B.W (%) | | | Loaded $Q_L$ | | | | | |
|---|---|---|---|---|---|---|---|---|---|---|---|---|
| | $f_L$ | $f_M$ | $f_U$ | $f_L$ | $f_M$ | $f_U$ | $f_L$ | $f_M$ | $f_U$ | $\varepsilon_r$ | $h$ (mm) | Size (mm$^2$) |
| [5] | 0.9 | 1.59 | 2.15 | 15.55 | 14.01 | 11.42 | 6.43 | 7.14 | 8.75 | 4.6 | 0.8 | 15.2 × 82.4 |
| [6] | 2.16 | 3.98 | 5.96 | 8.79 | 23.4 | 14.1 | 11.37 | 4.28 | 7.10 | 10.2 | 1.27 | 32 × 12 |
| [7] | 2.04 | 2.87 | 3.97 | 12.5 | 11.8 | 13.9 | 7.85 | 8.44 | 7.22 | | | 10 × 5 |
| [8] | 2.5 | 3.2 | 4.7 | 5.2 | 12.2 | 11.3 | 19.2 | 8.2 | 8.8 | 10.2 | 1.27 | 25.6 × 16 |
| [9] | 2.37 | 3.54 | 5.01 | 6.33 | 3.95 | 3.79 | 15.8 | 25.3 | 26.4 | 2.55 | 1.5 | 41.6 × 8.4 |
| [10] | 2.56 | 3.42 | 4.08 | 12.1 | 2.93 | 2.45 | 8.26 | 34.2 | 40.2 | 10.2 | 1.27 | 31.2 × 16.2 |
| [11] | 2.36 | 3.48 | 5.16 | 6.36 | 9.19 | 8.67 | 15.73 | 10.87 | 11.53 | 2.2 | 1.575 | 21.1 × 9.1 |
| [12] | 2.59 | 6.38 | 10.67 | 46.28 | 16.22 | 8.05 | 2.13 | 5.21 | 11.48 | 2.52 | 0.504 | 20 × 6.4 |
| [13] | 2.4 | 3.4 | 5.8 | 34.5 | 16.7 | 9.0 | 2.89 | 5.98 | 11.11 | 10.2 | 1.27 | 36.9 × 18 |
| [14] | 1.98 | 5.6 | 7.78 | 41.92 | 14.28 | 25.02 | 2.39 | 7.0 | 4.0 | 2.52 | 0.504 | 20 × 5.2 |
| Case1 | 2.0 | 3.86 | 5.42 | 20.0 | 3.10 | 1.48 | 5.0 | 32.16 | 67.75 | 3.2 | 0.762 | 10 × 10 |
| Case2 | 1.6 | 2.94 | 5.32 | 12.5 | 2.72 | 1.88 | 8.0 | 36.75 | 53.2 | 3.2 | 0.762 | 10 × 10 |
| Case3 (Sim) | 2.2 | 4.15 | 5.53 | 19.54 | 3.13 | 1.27 | 5.12 | 31.92 | 79.0 | 3.2 | 0.762 | 10 × 10 |
| **Case3 (mea)** | 2.19 | 4.14 | 5.53 | 19.10 | 3.86 | 1.62 | 5.21 | 25.87 | 61.44 | 3.2 | 0.762 | 10 × 10 |

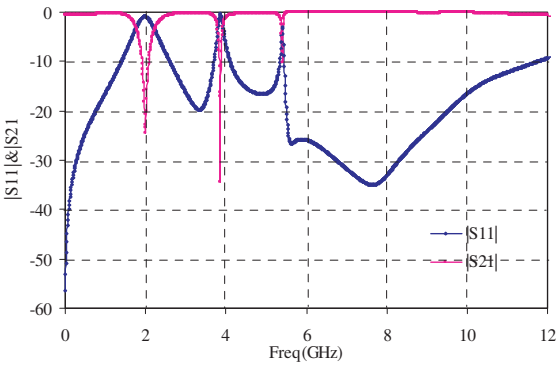


**Figure 5.** $|S_{11}|$ and $|S_{21}|$ of Triple-Band BSF for $f_1 = 2.0$ GHz, $f_2 = 5.42$ GHz and $f_3 = 3.86$ GHz (case-1).

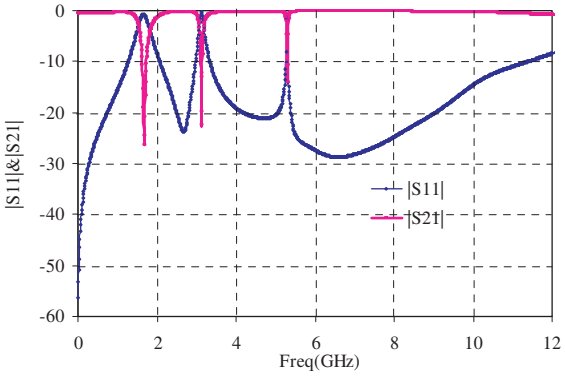


**Figure 6.** $|S_{11}|$ and $|S_{21}|$ of Triple-Band BSF for $f_1 = 1.6$ GHz, $f_2 = 5.32$ GHz and $f_3 = 2.94$ GHz (case-2).

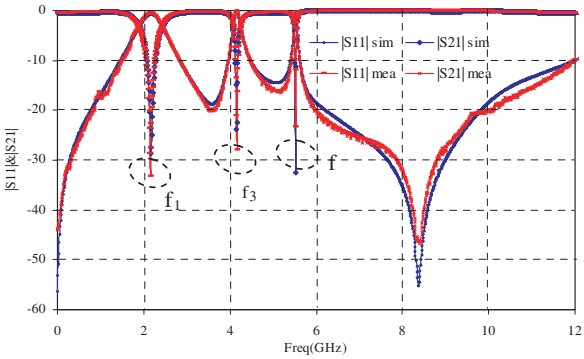


**Figure 7.** Simulated and measured $|S_{11}|$ and $|S_{21}|$ of Triple-Band BSF for $f_1 = 2.2\,\text{GHz}$, $f_2 = 5.53\,\text{GHz}$ and $f_3 = 4.15\,\text{GHz}$ (case-3).

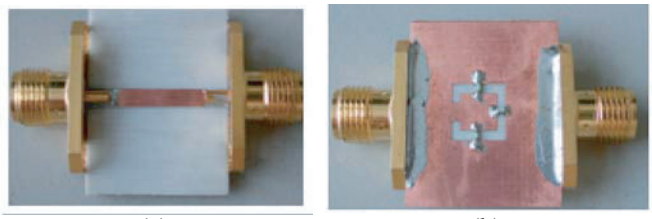

(a) (b)

**Figure 8.** Fabricated Triple-Band BSF for $f_1 = 2.2\,\text{GHz}$, $f_2 = 5.53\,\text{GHz}$ and $f_1 = 4.15\,\text{GHz}$ on $\varepsilon_r = 3.2$, $h = 0.762\,\text{mm}$. (a) Top side. (b) Bottom side.

## 4. CONCLUSION

A very compact Triple-Band BSF using embedded chip capacitors has been designed and fabricated for frequencies 2.2 GHz, 5.53 GHz and 4.15 GHz with attenuation levels 33.5 dB, 27.6 dB and 24.9 dB. Insertion losses (IL) between the stop bands are between 0.08 and 0.09 dB. Design charts are also developed to design the TB-BSFs. Such a type of filter can be useful for the modern microwave communication system to suppress unwanted signal frequencies from the WLAN and UWB band.

## ACKNOWLEDGMENT

This work is supported by the Delhi University Innovation Project 2015–2016. The authors also want to acknowledge Prof. B. K. Kanojia of Department of ECE, Ambedkar Institute of Advanced Communication Technologies and Research, Geeta Colony, Delhi 110031, India, for providing the measurement facility.

## REFERENCES

1. Uchinda, H., H. Kamino, K. Totani, N. Yoneda, M. Miyazaki, Y. Konishi, S. Makino, J. Hirokawa, and M. Ando, "Dual-band-rejection filter for distortion reduction in RF transmitters," *IEEE Trans. Mirow. Theory Tech.*, Vol. 52, No. 11, 2550–2556, Nov. 2004.
2. Chin, K. S., J. H. Yeh, and S. H. Chao, "Compact dual-band bandstop filters using stepped-impedance resonators," *IEEE Microw. Wireless Component Lett.*, Vol. 17, No. 12849-851, Dec. 2007.
3. Chiou, H. K. and C. F. Tai, "Dual-band microstrip bandstop filter using dual-mode loop resonator," *Electronic Lett.*, Vol. 45, No. 10, 507–509, May 2009.

4. Verma, A. K., A. Abdel-Rahman, A. Kumar, A. Balalem, and A. Omar, "New compact dual-band bandstop filter," *International Journal of Electronics*, Vol. 100, No. 4, 497–507, Taylor & Francis, 2013.
5. Liao, S.-S., S.-Y. Yuan, Y.-L. Wu, and T.-Y. Huang, "Compact microstrip bandstop filter with controllable triple stopband response," *PIERS Proceedings*, 1377–1380, Kula Lumper, Malaysia, Mar. 27–30, 2012.
6. Xiao, J.-K. and Y.-F. Zhu, "Multiband bandstop filter using inner t-shaped defected microstrip structure (DMS)," *International Journal of Electronics and Communication (AEU)*, Vol. 68, 90–96, 2014.
7. Chiu, L. and Q. Xue, "A simple microstrip bandstop filter using cross-coupling stubs," *International Journal of Microwave Science and Technology*, Article ID 473030, 2012.
8. Xiao, J. K. and H. F. Huang, "Square patch resonator banstop filter," *12th IEEE International Conference on Communication Technology (ICCT)*, 104–107, Nov. 11–14, 2010.
9. Ning, H., J. Wang, Q. Xiong, and L.-F. Mao, "Design of planar dual and triple narrow-band bandstop filters with independently controlled stopbands and improved spurious response," *Progress In Electromagnetics Research*, Vol. 131, 259–274, 2012.
10. Xiao, J.-K. and Y.-F. Zhu, "New U-shaped DGS bandstop filters," *Progress In Electromagnetics Research C*, Vol. 25, 179–191, 2012.
11. Jankovic, N., R. Geschke, and V. C. Bengin, "Compact tri-bnad bandpass and bandstop filters based on Hilbert-Fork resonators," *IEEE Microwave and Wireless Components Letters*, Vol. 23, No. 6, Jun. 2013.
12. Dhakal, R. and N. Y. Kim, "A compact systematic microstrip filter based on a rectangular meandered line stepped impedance resonator with a triple band bandstop response," *The Scientific World Journal*, Vol. 2013, Article ID 457693, 2013.
13. Sassi, I., L. Talbi, and K. Hettak, "Compact multi-band filter based on multi-ring complementary split ring resonators," *Progress In Electromagnetics Research C*, Vol. 57, 127–135, 2015.
14. Koirala, G. R. and N.-Y. Kim, "Multiband bandstop filter using an i-stub-loaded meandered defected microstrip structure," *Radioengineering*, Vol. 25, No. 1, Apr. 2016.
15. FCC DA 13-1193, May 2013.
16. CST Microwave Studio, 2011.